Atomistic modeling of impurity ion implantation in ultra-thin-body Si devices

L. Pelaz[1], R. Duffy[2], M. Aboy[1], L. Marques[1], P. Lopez[1], I. Santos[1], B. J. Pawlak[2], M. J. H. van Dal[2],
B. Duriez[2], T. Merelle[2], G. Doornbos[2], N. Collaert[3], L. Witters[3], R. Rooyackers[3], W. Vandervorst[3],
M. Jurczak[3], M. Kaiser[4], R. G. R. Weemaes[4], J. G. M. van Berkum[4], P. Breimer[4], R. J. P. Lander[2]

[1]University of Valladolid, Valladolid, Spain. Tel: +34 983 185502, Fax: +34 983 423675, Email: lourdes@ele.uva.es
[2]NXP-TSMC Research Center, Leuven, Belgium,
[3]IMEC, Leuven, Belgium, [4]Philips Research Laboratories, Eindhoven, Netherlands.

Abstract

Source/drain formation in ultra-thin body devices by conventional ion implantation is analyzed using atomistic simulation. Dopant retention is dramatically reduced by backscattering for low-energy and low-tilt angles, and by transmission for high angles. For the first time, Molecular Dynamics and Kinetic Monte Carlo simulations, encompassing the entire Si body, are applied in order to predict damage during implant and subsequent recovery during anneal. These show that amorphization should be avoided as recrystallization in ultra-thin-body Si leads to twin boundary defects and poly-crystalline Si formation, despite the presence of a mono-crystalline Si seed. Rapid dissolution of end-of range defects in thin-body Si, caused by surface proximity, does not significantly reduce diffusion lengths. The conclusions of the atomistic modeling are verified by a novel characterization methodology and electrical analysis.

Introduction

The scaling of Si devices foresees the progressive reduction of the Si layer thickness for fully-depleted planar devices, and subsequently the transition to multi-gate devices with very narrow fin structures in order to control short channel effects (SCE). A major challenge is the increase in parasitic source-drain (S/D) resistance (R_{SD}) as the Si thickness (t_{Si}) is scaled (1,2). Conventional ion implantation is the preferred approach for S/D formation, but the inherent difficulties related to damage generation, enhanced dopant diffusion and activation are aggravated by the small tilt angles required to avoid resist shadowing in dense fin pitches (3) and by the difficulty to regrow thin Si layers (4).

In this work we use atomistic simulation techniques such as classical Molecular Dynamics (MD) and Kinetic Monte Carlo (KMC) to gain physical understanding of the mechanisms involved in impurity ion implantation in ultra-thin body Si devices and provide insight for process optimization. The combined application of MD and KMC modeling techniques to simulate device dimensions and to optimize process parameters is a key advance.

Dopant retention in fin structures

Highly tilted implants are required to incorporate the dopants along the fin structure but only a fraction of implanted dopants are retained (3). The different sources of dopant loss during FinFET extension implant are shown schematically in Fig. 1. Fig. 2 shows the retained dose vs implant angle for a typical range of B and As ultra-shallow implants, predicted from atomistic simulations using MARLOWE. For 10º implants backscattering causes significant dopant loss at low energies. For 45º implants impurity atoms are lost through the opposite fin side when high implant energies are used. The

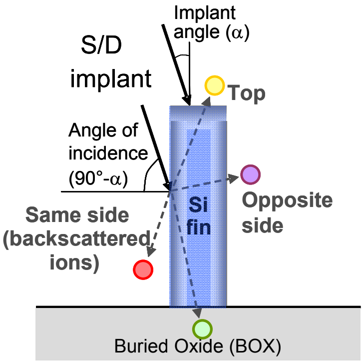

Fig.1. Schematic for different sources of dopant loss in sidewall implantation.

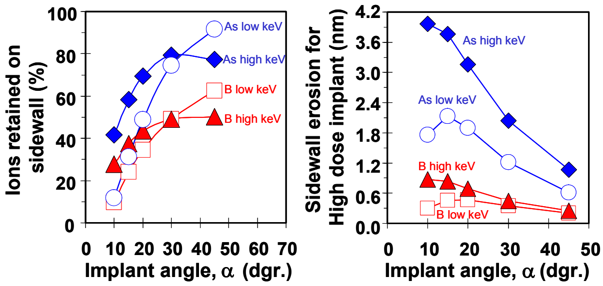

Fig. 2. Simulated B and As sidewall dose retention vs angle in a 10 nm wide fin (left) and estimated erosion depth (from simulated sputtering yield) for high dose implant vs angle (right). Small angle variations cause large changes in retention for small angles.

high slope of Fig. 2 when the tilt angle is small indicates that small variations in tilt angle (e.g. tapered surfaces, roughness) cause significant changes in the retained dose, and therefore influence device variability. Fig. 2 also includes the estimated erosion depth versus implant angle for a high dose implant. Erosion due to sputtering effects for highly oblique incident angles limits the maximum implant dose. Secondary Ion Mass Spectroscopy (SIMS) analysis through fin arrays is performed using the test structure shown in Fig. 3. The SIMS analysis of a 200 nm tall fin array, shown in Fig. 4, corroborates the inefficient dopant incorporation for low-energy low-tilt implants. Fig. 5 shows resistor experimental data versus the thickness of the fin (W_{fin}). For 10° implants the inefficient incorporation of dopant atoms must be compensated by increasing the implant dose. For 45° implants, resistance is improved by a reduction of implant energy.

Key in MOSFET extension optimization is the tradeoff between drive current and SCE control. 3D device simulation data in Fig. 6 shows, for fully-depleted FinFETs, drive current and SCE control are more sensitive to dose retention on sidewalls than to dopant conformality.

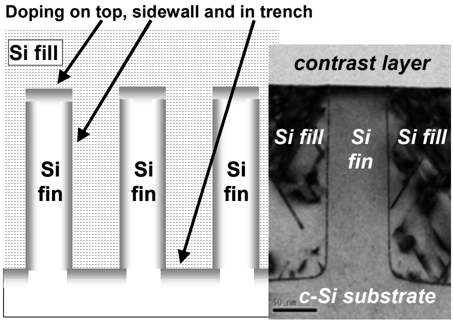

Fig. 3. Schematic and XTEM image of the fin array test structure used for SIMS characterization of the sidewall doping.

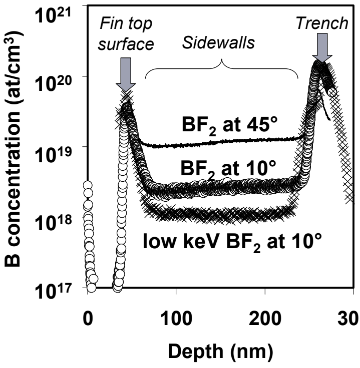

Fig. 4. SIMS analysis through fin arrays. The plateau indicates sidewall doping. Low-energy low-tilt implants produce poor dose retention.

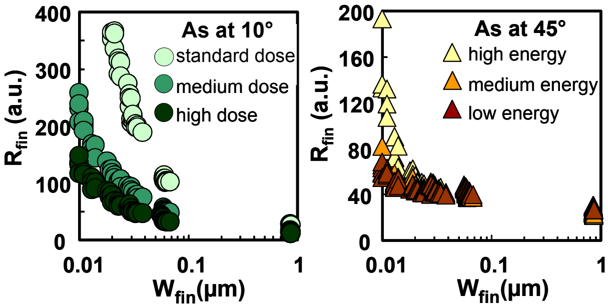

Fig. 5. Experimental fin resistance (R_{fin}) vs W_{fin} determined from a resistor experiment. High doses are required to optimize 10° tilts (left). High implant energies are bad at 45° tilts (right).

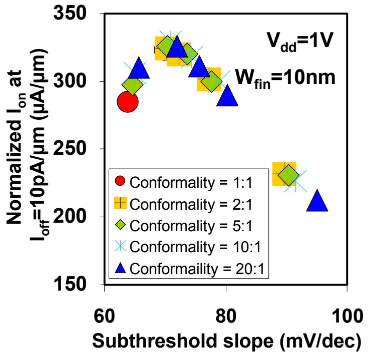

Fig. 6. 3D device simulation of drive at fixed off current vs SCE control. Trends are independent of doping conformality.

Amorphization and recrystallization issues

Amorphization and recrystallization in ultra-thin-body Si devices has become a pressing concern (1,2,4-6). A detailed atomistic amorphization model based on the accumulation of Interstitial-Vacancy (IV) pairs (7) is used to analyze damage accumulation and the kinetics of the crystalline to amorphous transition. MD simulations indicate that IV pairs located close to surfaces are more stable than those in bulk (8). The suppression of I-V recombination near the interfaces, along with the slow regrowth in the ‹111› direction, causes the formation of twin boundaries and polycrystals in thin-body devices oriented along ‹110› (4,5). This is illustrated in the MD simulation results of Fig. 7 and in the cross-sectional Transmission Electron Microscopy (XTEM) images of Fig. 8.

For implant at temperatures above the critical value IV-pairs dynamically anneal out (7). Therefore, amorphization and problems related to imperfect regrowth are prevented. The critical temperature increases with ion mass because heavier ions produce denser and more stable damage. In the case of p-type regions, BF_2 could be substituted by B since this does

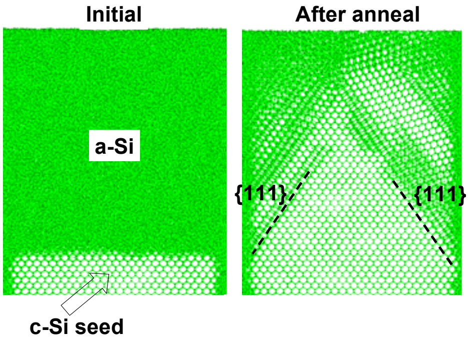

Fig. 7. Initial and final configurations in a MD recrystallization simulation of a ‹110› thin body Si. Regrowth produces ‹111› twinning.

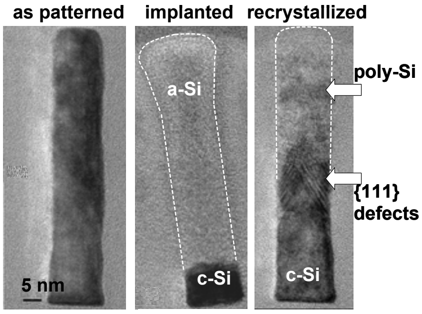

Fig. 8. XTEM showing amorphization & recrystallization produces many defects and even poly-crystalline silicon in thin-body Si.

not amorphize Si at room temperature (RT). However, n-type dopants are heavier and their critical amorphization temperature is above RT. Experimental data in Fig. 9 shows that amorphization can be completely prevented at implant temperatures in the order of 150 ºC for P and around 300ºC for As. Experimental dopant profiles show little difference between RT and raised wafer temperatures after spike Rapid Thermal Anneal (RTA). Simulation results in Fig. 10 indicate that a large amount of excess Si interstitials remains in end of range (EOR) defects as the amorphous/crystalline (a/c) interface depth is reduced. Intense dynamic anneal during implant can reduce the number of residual interstitials, but a larger number of interstitial hops at high temperatures, mostly during implant, implies significant dopant diffusion (9).

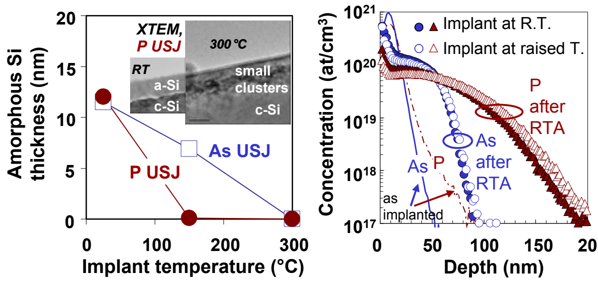

Fig. 9. Experimental analysis (left) shows at raised implant temperatures amorphization is prevented but a large number of defects remain. SIMS of As and P implanted at RT and at raised wafer temperatures (right). After RTA the junction depth is not significantly different.

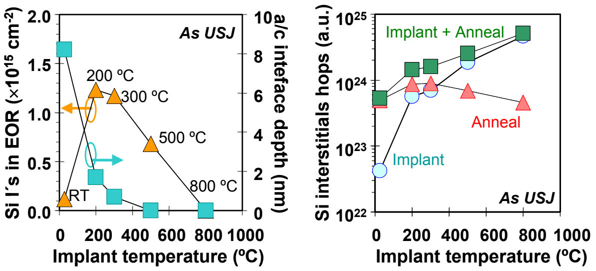

Fig. 10. Simulated a/c interface depth and EOR damage vs implant temperature (left). A reduced a/c depth may result in more residual defects. Simulated Si interstitial hops vs implant temperature, during implant and RTA anneal (right). More hops mean more diffusion.

Poor regrowth of amorphous regions degrades device performance, but regrowth improves if low amorphizing conditions are used. Fig. 11 shows that experimental NMOS and PMOS R_{SD} increase sharply for narrow W_{fin} but low amorphizing extension conditions dramatically reduce resistance. Fig. 12 shows the on-state current (I_{ON}) versus

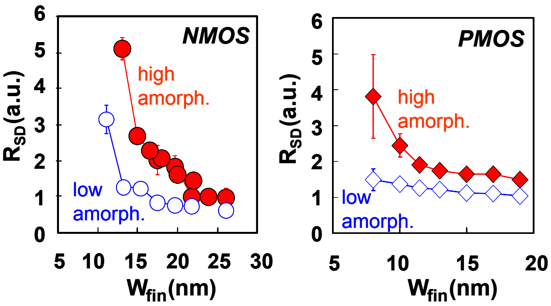

Fig. 11. Experimental NMOS (left) and PMOS (right) R_{SD} vs W_{fin}. Low amorphization improves R_{SD} for narrow W_{fin}. R_{SD} was extracted by plotting drive current (at V_{ds}=50 mV, V_{gs}=3 V) vs physical L_{gate} and extrapolating to 0 nm

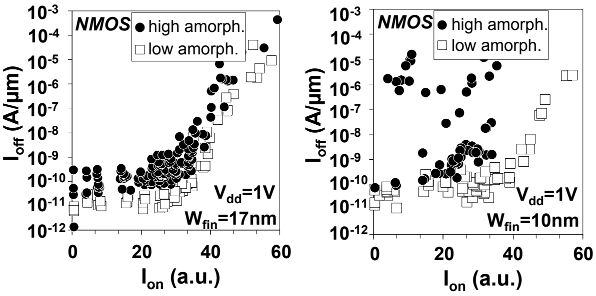

Fig. 12. Experimental NMOS Ion vs Ioff, for W_{fin} =17 nm (left) and W_{fin}=10 nm (right). Performance is comparable for high and low amorphizing conditions for wide fins (left). Drive is maintained with low amorphizing conditions, and not for high amorphizing conditions for narrow fins (right).

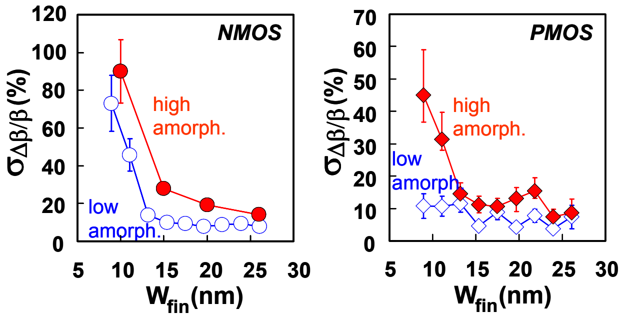

Fig. 13. Experimental NMOS (left) and PMOS (right) σΔβ/β vs W_{fin}, from matching pairs (L_g=35 nm), is better with low amorphization.

off-state current (I_{OFF}) for NMOS devices. For relatively wide fins the performance is comparable for high and low amorphizing conditions. For thin fins the benefit of low amorphization becomes obvious. The impact of extension conditions on local mismatch is demonstrated in Figs. 13. The gain mismatch (σΔβ/β) is also improved by low amorphization.

Dopant diffusion and activation

In ultra-thin-body devices the proximity of defects to surfaces favors their rapid annihilation and the fast recovery to equilibrium conditions. Fig. 14 compares the simulated residual defects after different thermal treatments for bulk and different fin structures. Lower thermal budget may be enough to eliminate defects resulting from preamorphizing conditions in thin Si structures compared to thicker ones. Simulations and SIMS profiles shown in Fig. 15 indicate that dopant diffusion and activation are not significantly altered because equilibrium conditions are achieved rapidly.

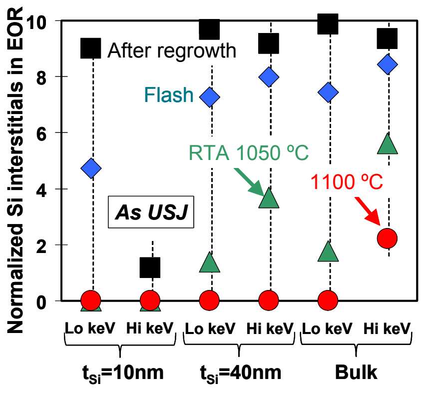

Fig. 14. Simulated EOR damage after different thermal treatments. Low thermal budgets can remove EOR damage in thin body Si structures.

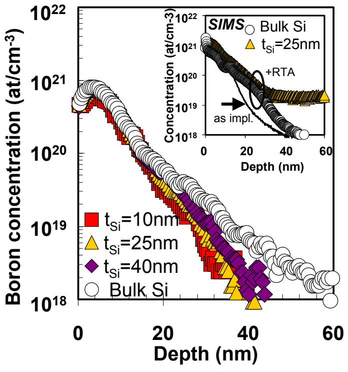

Fig. 15. Simulated B concentration vs depth (SIMS in inset), shallow implant followed by RTA anneal. Diffusion is similar for different t_{Si}.

Conclusions

A detailed understanding of the dynamics of dopant engineering in ultra-thin-body Si is enabled by classical MD and KMC calculations. Trade-offs between tilt angle, energy and dose during implant are studied in detail and implantation at elevated temperatures is evaluated. The proximity of interfaces favors the removal of EOR defects even with small thermal budgets. Poor regrowth of amorphous layers degrades device performance and low amorphizing implant conditions are critical for scaling of thin-body Si devices.

Acknowledgments

This work has been partially funded by the European PULLNANO Integrated Project (FP6 – IST-026828) and by the Spanish Ministry of Education (Project TEC2005-05101).

References

(1) J. Kedzierski *et al.*, “Extension and source/drain design for high-performance FinFET devices”, *IEEE Trans .Electron Devices*, vol. **50**, pp. 952-958, April 2003.

(2) M. J. H. van Dal *et al.*, “Highly manufacturable FinFETs with sub-10nm fin width and high aspect ratio fabricated with immersion lithography,” *Symp. VLSI Tech. Dig.*, 2007, pp. 110-111.

(3) R. Duffy *et al.*, “Doping fin field-effect transistor sidewalls: Impurity dose retention in silicon due to high angle incident ion implants and the impact on device performance”, *J. Vac. Sci. Technol. B*, vol. 26, pp. 402-407, 2008.

(4) R. Duffy *et al.*, “Solid phase epitaxy versus random nucleation and growth in sub-20 nm wide fin field-effect transistors”, *Appl. Phys. Lett.*, vol. 90, 241912, 2007.

(5) Y. Kunii, M. Tabe and K. Kajiyama, “Amorphous-Si crystalline-Si facet formation during Si solid-phase epitaxy near Si/SiO2 boundary”, *J. Appl. Phys.*, vol. 56, pp. 279-285, 1984.

(6) K. Saenger *et al.*, “Effect of Elevated Implant Temperature on Amorphization and Activation in As-implanted Silicon-on-insulator Layers” Mat. Res. Soc. Spring Meeting Symp. E Proc., 1070-E05-02, 2008.

(7) L. Pelaz, L.A. Marqués and J. Barbolla, “Ion-beam-induced amorphization and recrystallization in silicon”, *J. Appl. Phys.*, vol. **96**, pp. 5947-5976, 2004.

(8) L. Pelaz, unpublished.

(9) V. C. Venezia *et al.*, “Radiation-enhanced diffusion of Sb and B in silicon during implantation below 400 ºC”, *Phys. Rev. B*, vol. 69, 125215, 2004.